Journal of
Materials Chemistry C

Accepted Manuscript

This is an *Accepted Manuscript*, which has been through the RSC Publishing peer review process and has been accepted for publication.

Accepted Manuscripts are published online shortly after acceptance, which is prior to technical editing, formatting and proof reading. This free service from RSC Publishing allows authors to make their results available to the community, in citable form, before publication of the edited article. This *Accepted Manuscript* will be replaced by the edited and formatted *Advance Article* as soon as this is available.

To cite this manuscript please use its permanent Digital Object Identifier (DOI®), which is identical for all formats of publication.

More information about *Accepted Manuscripts* can be found in the **Information for Authors**.

Please note that technical editing may introduce minor changes to the text and/or graphics contained in the manuscript submitted by the author(s) which may alter content, and that the standard **Terms & Conditions** and the **ethical guidelines** that apply to the journal are still applicable. In no event shall the RSC be held responsible for any errors or omissions in these *Accepted Manuscript* manuscripts or any consequences arising from the use of any information contained in them.

RSC Publishing

www.rsc.org/materialsC
Registered Charity Number 207890

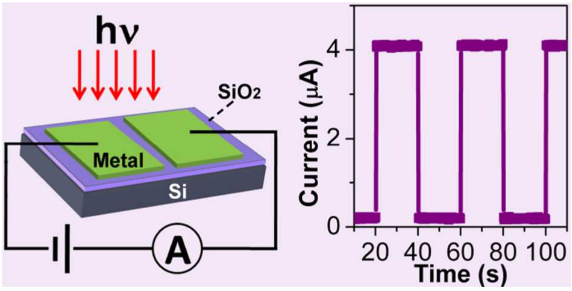

Metal/SiO_2/Si planar photodetectors with superior performance were fabricated conveniently and cost-effectively utilizing leakage current flows through SiO_2 layer.

Cite this: DOI: 10.1039/c0xx00000x

www.rsc.org/xxxxxx

PAPER

Simple Metal/SiO_2/Si Planar Photodetector Utilizing Leakage Current Flows through SiO_2 Layer

Baiyi Zu,[a] Bin Lu,[a] Yanan Guo,[a] Tao Xu[b] and Xincun Dou*[a]

Received (in XXX, XXX) Xth XXXXXXXXX 20XX, Accepted Xth XXXXXXXXX 20XX

DOI: 10.1039/b000000x

Silicon wafers covered with a thermally grown high-quality SiO_2 layer were often used as the substrate to house different nanostructures to fabricate photodetection devices. No reports have ever challenged to directly fabricate photodetectors utilizing leakage current through non-high-quality SiO_2 film and the intrinsic light absorption properties of Si. Herein, we show that metal/SiO_2/Si planar photodetectors could be easily fabricated by simply depositing two metal electrodes (such as, Au, Ag and Al) on top of SiO_2/Si wafer in which the SiO_2 layer is of non-high-quality. The responsivity, stability, photoresponse characteristics and light intensity sensitivity are systematically evaluated. Our results clearly show that the present conveniently and cost-effectively fabricated metal/SiO_2/Si planar photodetectors are of great advantage compared to many of the nanostructure-based photodetectors constructed on SiO_2/Si substrate.

Introduction

Photodetection devices based on nanostructured materials, e.g. inorganic 1-D nanowires, [1-7] polymers, [8, 9] and two dimensional graphene [10] often use silicon wafers covered with a thermally grown SiO_2 layer (typically 100~600nm thick) as the substrate to house the electric circuits. Usually, the insulation of the SiO_2 is the first important condition in the community of making photodetectors on the SiO_2/Si substrate (e.g. nanowire detectors on SiO_2/Si). [11-15] It is generally considered that if the top SiO_2 layer is of high-quality and over 200 nm thick, it is insulating enough to eliminate any electrical contribution from the underneath Si layer. And it is common sense that there will be leakage current if non-high-quality SiO_2 film is adopted. However, is it a possible way to directly fabricate photodetectors utilizing non-high-quality top SiO_2 layer since Si is broadly used in photovoltaic devices? [16-28] No reports have ever challenged this issue.

Herein, we show that metal/SiO_2/Si planar photodetectors could be easily fabricated by simply depositing two metal electrodes on top of SiO_2/Si wafer. We observed remarkable photocurrent between the two electrodes when the SiO_2 layer is ~200 nm thick. There are two advantages in this design to be highlighted. First, compared to the most common silicon-based photodiodes, which convert optical signals into electrical signals by means of optical absorption followed by charge separation across a p-n junction, and silicon transistors, which produce electrical readout,[29, 30] the fabrication of the current metal/SiO_2/Si planar photodetectors is convenient and cost-effective. Second, compared to many of the nanostructure-based photodetectors constructed on SiO_2/Si substrate, it is of high stability and of superior performance.

Experimental section

The SiO_2(200±15 nm thick)/Si<111>(p-type, resistance <1Ω • cm) wafer was washed by ultrasonication in deionized water, acetone and ethanol in sequence for 15 min, respectively. The wafer was wrapped along all the edges by thermal tape to avoid the direct conduction. The gold electrode was sputtered with a compact plasma sputtering coater (GSL-1100X-SPC-12, MTI Corporation, vacuum pressure 7×10^{-3} Pa, sputtering current 8 mA and coating time 40 s) to get Au/SiO_2/Si photodetector. Al film was coated by thermal evaporation. Field-emission scanning electron microscopy (FESEM, ZEISS SUPRA 55VP) was used to characterize the cross section of the SiO_2/Si wafer. Atomic force microscopy (AFM, MultiMode 8, BRUKER) was used to characterize the morphology and the thickness of the gold electrodes.

The Quantum Efficiency (QE) of Au/SiO_2/Si photodetector was recorded by Oriel Quantum Efficiency Measurement Kit (UV-Si photodiode sensor: 71675; power meter: 2936-R; monochromator: 74125) by measuring a dc current at different wavelengths from 300 to 1100 nm using a xenon lamp (300W 6258). The current–voltage characteristics and the photocurrent response were recorded in ambient atmosphere by a ZAHNER ZENNIUM potentiostat. Field effect transistor characteristics were measured by applying different gate voltages at the back side Si wafer. The illuminated light intensity was modulated by a Controlled Intensity Modulated Photocurrent Spectrometer (CIMPS-2, ZAHNER) system. The data acquisition frequency is 5 Hz. The light wavelength was controlled by a switchable light emitting diode (LED, BUVZ02) light source.

Results and discussion

The schematic diagram of the obtained Au/SiO_2/Si photodetector is illustrated in Figure 1a. The thickness of SiO_2 layer is confirmed to be around 200 nm by imaging the cross section of

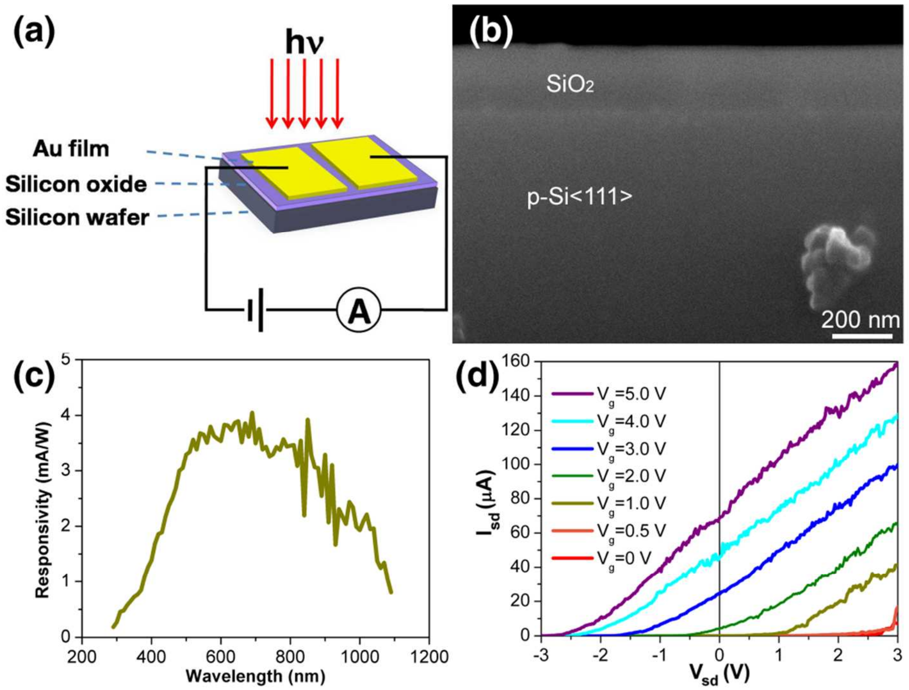

Fig. 1 (a) Schematic diagram of the obtained Au/SiO_2/Si photodetector, (b) SEM image of the cross section of SiO_2/Si substrate, (c) Responsivity of the Au/SiO_2/Si photodetector, and (d) I_{sd} – V_{sd} plots at different V_g of the corresponding back side gate field effect transistor.

the SiO_2/Si wafer using a scanning electron microscopy (SEM) (Figure 1b). The channel length is 40 μm and the channel width is 5 mm (Figure S1). The thickness of the sputtered gold electrode is ~12 nm measured by atomic force microscopy (AFM) (Figure S2). The Au film exhibits good conductivity as an electrode (Figure S3). External quantum efficiency (EQE) of Au/SiO_2/Si substrate as a photodetector was obtained by measuring a dc current at different wavelengths from 300 to 1100 nm (Figure S4). The external quantum efficiencies are 0.27%, 0.55% and 0.71% at 367, 426 and 468 nm, respectively. Figure 1c displays the photocurrent response of the two Au electrodes on SiO_2/Si substrate by measuring a dc current illuminated at different wavelengths from 300 to 1100 nm. The responsivity was calculated from the measured external quantum efficiency (Figure S4) by the following formula:

$$R_\lambda = EQE \cdot \lambda e/hc$$

where R_λ is the responsivity, λ is the excitation wavelength, *e* is electron charge, *h* is Planck's constant and *c* is speed of light in vacuum. The responsivity curve peak of the present Au/SiO_2/Si photodetector showed an obvious blue shift to 500-700 nm, comparing with the typical responsivity curves of silicon photodetectors which have peak values from 700 to 1000 nm (Figure S5 and Figure S6). We think that the existence of the SiO_2 layer blocked those low-energy photoelectrons (<1.77 eV, corresponding to 700 nm), as can be evidenced by the plots of Lnσ *versus* 1/T for Au/SiO_2/Si photodetector in dark and under light illumination taking Au/Si substrate as the reference (Figure S7). The I_{sd} – V_{sd} plots at different V_g of the corresponding back side gate field effect transistor is shown in Figure 1d. One can see that the source-drain current at an applied voltage of zero keeps increasing with the increase of the gate voltage, indicating the existence of leakage current in SiO_2 layer.

Figure 2a shows the current-voltage (I–V) characteristics of an Au/SiO_2/Si photodetector in dark condition and under illumination of three different lights with wavelengths of 367 nm, 426 nm and 468 nm, respectively. The light intensities of all the three light sources are 0.8 mW/cm^2. The I–V curves display a nonlinear behavior in a voltage range from -2 V to 4 V. An enhancement of current has been observed when the device was illuminated. At a fixed voltage of 4 V, the photocurrent illuminated by 468 nm light (28.9 μ A), 426 nm light (35.8 μA) and 367 nm light (41.5 μA) was about 1.6, 1.9 and 2.2 times of the dark current (18.6 μA), respectively. This can be explained as that high energy photons can produce high energy electrons and thus contribute more to the photocurrent. [15] Photosensitivity was calculated according to the I–V characteristics of the photodetector illuminated at 367 nm shown in Figure 2a, as shown in Figure S8a. The detecvity can be expressed as: [31]

$$D^* = (J_{\mathrm{ph}}/L_{\mathrm{light}})/(2qJ_{\mathrm{d}})^{1/2}$$

where q is the absolute value of electron charge (1.6×10^{-19} Coulombs), J_{ph} and J_{d} are the photocurrent and dark current respectively, L_{light} is the light intensity. Detectivity was calculated according to the I–V characteristics of the photodetector illuminated at 367, 426 and 468 nm shown in Figure 2a, as shown in Figure S8b. Detecivities were calculated using this equation at λ= 367, 426 and 468 nm. With a bias of 2 V, $D^*=1.01\times10^{10}$ Jones, 1.33×10^{10} Jones and 1.50×10^{10} Jones for illumination at λ= 468, 426 and 367 nm, respectively. Furthermore, we observed that the I-V curves in Figure 2a are asymmetric, i.e., the current under forward bias is always higher than the one under reverse bias with the same absolute value of voltage. We think the

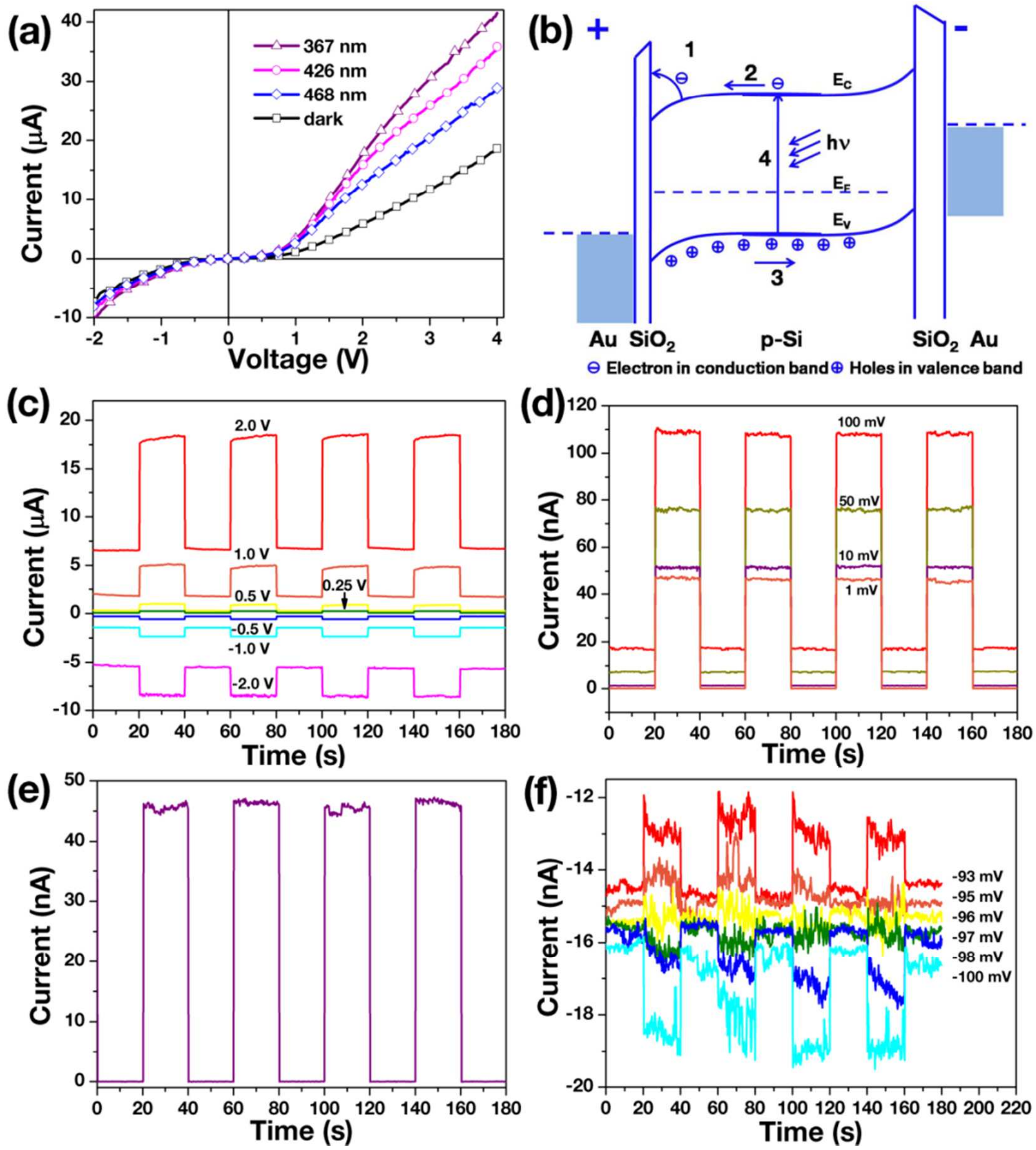

Fig. 2 (a) I–V characteristics of an Au/SiO_2/Si photodetector in dark condition and illuminated with different wavelength lights (0.8 mW/cm^2). (b) Energy-band diagram (not to scale) of the Au/SiO_2/Si photodetector under forward bias. The basic charge transport mechanisms shown are (1) electrons thermionic emission; directional transport of (2) electrons in the conduction band and (3) holes in the valence band, (4) light absorption induced electron excitation from valence band to conduction band. E_C, E_V, and E_F are the conduction band minimum, the valence band maximum, and the Fermi level, respectively; $h\nu$ represents the illuminated light. Time-dependent photoresponse of the Au/SiO_2/Si photodetector measured by periodically turning on and off a 367 nm light (0.8 mW/cm^2) at different biases (c, d) from -2 V to 2 V, (e) 0 V and (f) -93 mV, -95 mV, -96 mV, -97 mV, -98 mV and -100 mV.

asymmetric I-V characteristic, which is further confirmed in Figure S9, is inevitable and is attributed to the asymmetric potential energy barrier caused by the difference either in the effective insulating layer thickness or in the tightness of the connection between the two Au electrodes and the SiO_2 layer. In other words, the barrier width of the left side SiO_2 layer is thinner than that of the right side SiO_2 layer.

Figure 2b shows the corresponding energy-band diagram (not to scale) of the Au/SiO_2/Si photodetector. In dark condition, thermionic emission electrons are dragged by the forward bias and some of them could flow through the 200 nm thick SiO_2 layer. The electrons in the conduction band were directionally transported to the left side SiO_2 interfacial layer and followed by flow through it and collected by the left gold electrode at a forward bias. At the same time, the holes in the valence band were directionally transported to the right side SiO_2 interfacial layer and recombined by the electrons flow through it from the right gold electrode. This is the origin of the generation of the dark current. [32] Since silicon is a semiconductor, and it absorbs light from ultraviolet to infrared (as shown in Figure 1c), under the illumination of the light whose photon energy is larger than the bandgap of silicon, the electrons were excited from the valence band to the conduction band. As a result, the number of the charge carriers was greatly increased and the photocurrent was generated. The corresponding photon energy of all the three light (2.65-3.38 eV) is much higher than the bandgap of Si (1.14

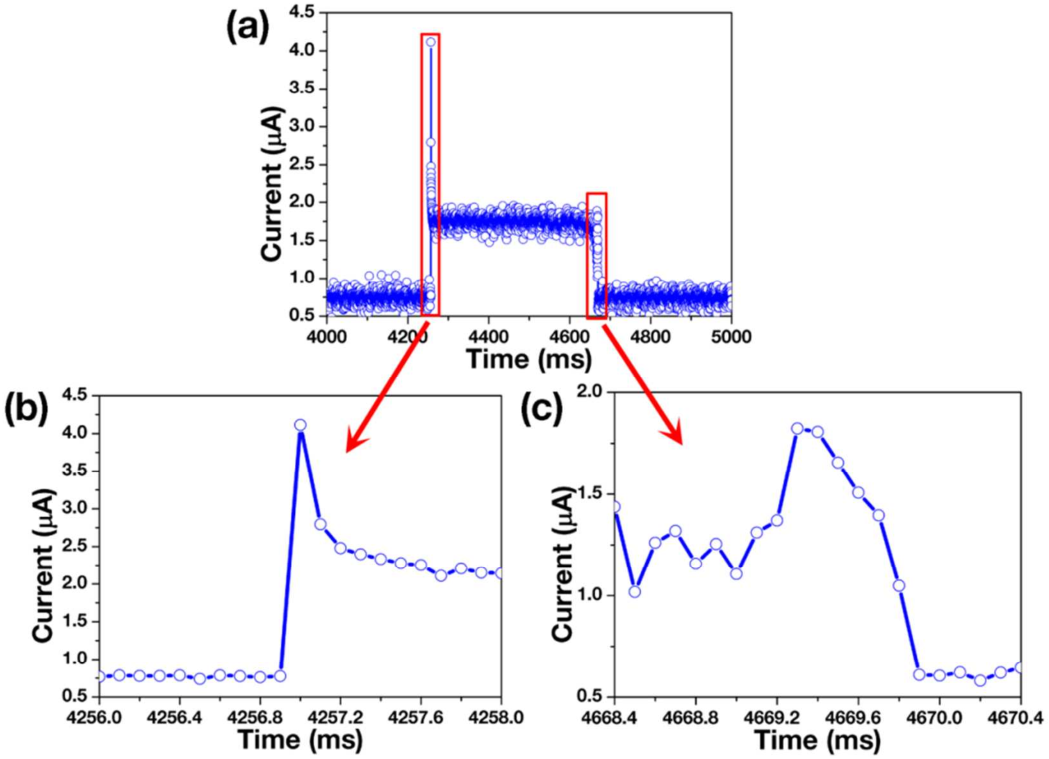

Fig. 3 (a) Time-dependent photoresponse of the Au/SiO_2/Si photodetector measured by periodically turning on and off a common flashlight at a forward bias of 2 V, the data acquisition frequency is 10 KHz. (b, c) the enlarged portions for 4256–4258 ms and 4668.4–4670.4 ms, which correspond to light-off to light-on and light-on to light-off processes, respectively.

eV), and thus the electrons in the valence band of Si could be excited by any of them.

To show the reproducibility, stability and the application requirements of the present photodetector, the time-dependent photoresponse of the Au/SiO_2/Si photodetector are measured by periodically turning on and off a 367 nm light at different biases. Upon illumination, the photocurrents rapidly increased to a stable value of 18.3, 5.2, 0.87, 0.25, -0.56, -2.3, -8.7 μA at a bias of 2.0 V, 1.0 V, 0.5 V, 0.25 V, -0.5 V, -1.0 V and -2.0 V, respectively, and then drastically decreased to its initial level when the light was turned off (Figure 2c), indicating the excellent stability and reproducible characteristics of the Au/SiO_2/Si photodetector. This superior performance could be observed even at very low biases of 1.0 mV, 10 mV, 50 mV and 100 mV (Figure 2d). The dark currents are 0.12 and 1.28 nA at a bias of 1 mV and 10 mV, and the ratios of photocurrent to dark current are 388 and 40, respectively. This result strongly suggests that the Au/SiO_2/Si photodetector is an excellent photodetector at very low biases, and could be driven by nanocell or 1-dimensional nanostructure based thermoelectric devices. [21, 33, 34] It should be noted that there is photoresponse in the photodetector with a SiO_2 thickness of 150 nm (Figure S10), but it is not as good as that shown in Figure 2c and 2d. There is no photoresponse in the device with a SiO_2 thickness of 300 nm (Figure S11), which is consistent with the previously reported results (ref. 15). There is no leakage current in the device with a SiO_2 thickness of 1000 nm (Figure S12).

Figure 2e shows the time-dependent photoresponse at a bias voltage of 0 V under 367 nm light illumination. The dark current is 0, while the photocurrent is about 46 nA. This result clearly showed that the Au/SiO_2/Si photodetector could realize the photodetecting function even without providing an external bias. We think this is due to the inevitable slight difference in the Au/SiO_2/Si interfaces at the two electrodes which limits the electron diffusion slightly differently. Figure 2f shows curves of photocurrent *versus* time at a bias around -96 mV. The absolute value of the photocurrent is lower than the absolute value of the dark current when the applied voltage is higher than -96 mV. While this trend was shifted once the applied voltage is lower than -96 mV. This result demonstrated that the reverse bias of -96 mV behaves like a “blind” point since the dark current is almost equal to the photocurrent at this voltage.

The time response speed is usually a key factor for sensor performance and it determines the capability of a photodetector to follow a fast-varying optical signal. Figure 3a shows the time-dependent photoresponse of the Au/SiO_2/Si photodetector measured by periodically turning on and off a common flashlight at a forward bias of 2 V. The enlarged portions for 4256–4258 ms and 4668.4–4670.4 ms respectively corresponding to light-off to light-on and light-on to light-off processes were shown in Figure 3b and 3c. One can see that the rise time is faster than the limit of the measurement setup (0.1 ms) since no other current values were observed between the photocurrent and the dark current. The decay time is around 0.2 ms.

The Au/SiO_2/Si photodetector is also quite sensitive upon very weak light illumination, for example, 0.1 mW/cm^2 (Figure S13). One can see that the photocurrent as a function of light intensity increases at a forward bias of 2 V, and it could be well fitted with a polynomial equation of the second degree.

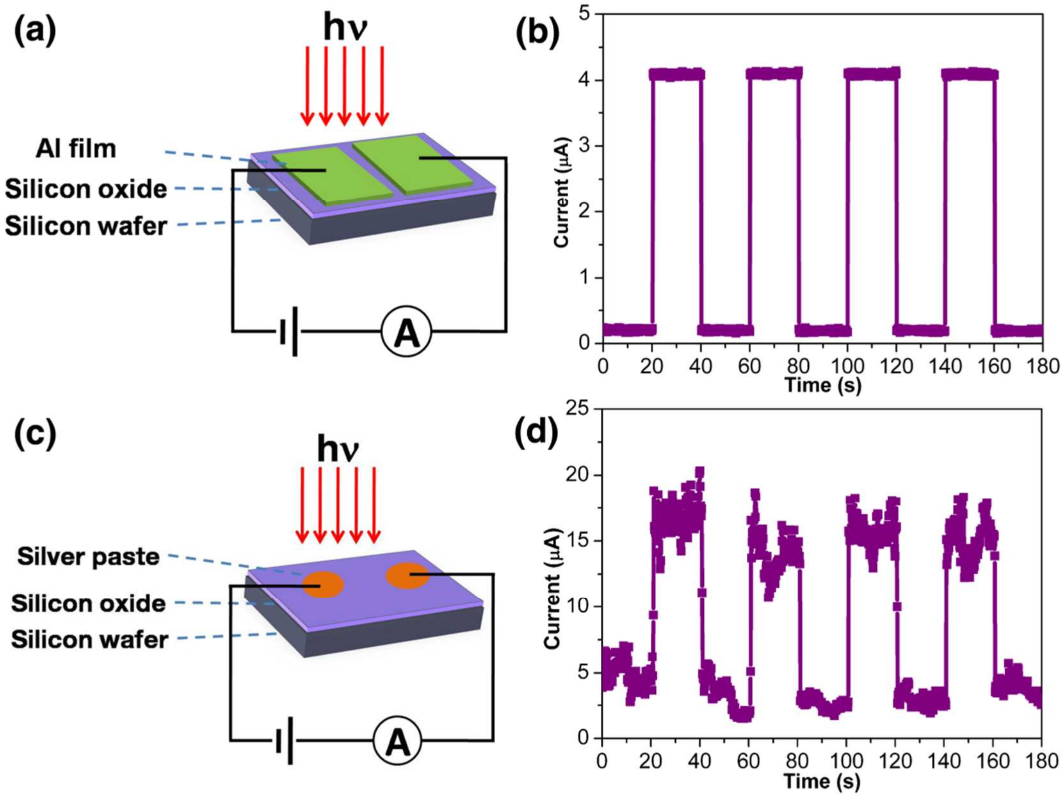

Fig. 4 (a) Schematic diagram of an Al/SiO_2/Si photodetector, the thicknesses of the SiO_2 layer and Al layer are 200±15 nm and 75 nm, respectively. (b) The corresponding photocurrent *versus* time at a bias of 2 V (367 nm, 0.8 mW/cm^2). (c) Schematic diagram of an Ag/SiO_2/Si photodetector, the thickness of the SiO_2 layer is 200±15 nm. (d) The corresponding photocurrent *versus* time at a bias of 2 V (367 nm, 0.8 mW/cm^2).

To show that other metal electrodes can also help to fabricate photodetectors on SiO_2/Si substrate, Al film and silver paste were fabricated on SiO_2/Si substrate. Figure 4a shows the schematic diagram of an Al/SiO_2/Si photodetector, the thicknesses of the SiO_2 layer and the evaporated Al layer are 200±15 nm and 75 nm, respectively. The corresponding photocurrent *versus* time at a bias of 2 V under 367 nm light illumination also shows a remarkable time-dependent photoresponse (Figure 4b). The photodetector fabricated by directly spreading silver paste on SiO_2/Si wafer as the electrodes (Figure 4c) also shows an obvious time-dependent photoresponse (Figure 4d). This result clearly demonstrated that the basic design of the present metal/SiO_2/Si photodetector is universal.

Conclusions

Planar metal/SiO_2/Si photodetectors were fabricated by simply depositing two metal electrodes (such as, Au, Ag and Al) on top of SiO_2/Si wafer in which the SiO_2 layer is of non-high-quality. It is found that the responsivity curve peak of the present Au/SiO_2/Si photodetector showed an obvious blue shift to 500-700 nm due to the existence of the SiO_2 layer which blocked the low-energy photoelectrons. It shows rapid and stable photoresponses. The rise time is less than 0.1 ms and the decay time is around 0.2 ms. It is highly sensitive to relatively weak light illumination (0.1 mW/cm^2) and works excellently at a low applied bias (1 mV). The generation of the photocurrent was attributed to the light absorption of silicon and the leakage in SiO_2 layer. Our results clearly show that the present conveniently and cost-effectively fabricated metal/SiO_2/Si planar photodetectors are of superior performance compared to many of the nanostructure-based photodetectors constructed on SiO_2/Si substrate. In perspective, this work might suggest those working on SiO_2/Si-substrated photodetectors that an evaluation on the substrate contribution is essential to understand the intrinsic properties of the aimed structure.

Acknowledgements

Financial supports by the National Natural Science Foundation of China (51372273, 51201180, 21204100), the “Hundred Talents Program" of Chinese Academy of Sciences (Y12H981601), the “Western Light” program of Chinese Academy of Sciences (LHXZ201102, XBBS201120), the International Scientific Cooperation Program of Xinjiang (20136008), “Xinjiang Science Foundation for Distinguished Young Scholars” (2013711015) and “Xinjiang Talent Plan” are gratefully acknowledged.

Notes and references

[a] *Laboratory of Environmental Science and Technology, Xinjiang Technical Institute of Physics & Chemistry; Key Laboratory of Functional Materials and Devices for Special Environments, Chinese Academy of Sciences, Urumqi 830011, China. Fax: +86-991-383-8957; Tel: +86-991-367-7875; E-mail: xcdou@ms.xjb.ac.cn*

[b] *Department of Chemistry and Biochemistry, Northern Illinois University, DeKalb, Illinois 60115, USA*

†Electronic Supplementary Information (ESI) available: [AFM characterization, quantum efficiency, temperature dependence, I-V characterization of Au/SiO_2/Si photodetectors/devices with different SiO_2 thickness and photoresponse calibration]. See DOI: 10.1039/b000000x/

1. J. Wang, M. S. Gudiksen, X. Duan, Y. Cui and C. M. Lieber, *Science*, 2001, **293**, 1455-1457.
2. C. Schliehe, B. H. Juarez, M. Pelletier, S. Jander, D. Greshnykh, M. Nagel, A. Meyer, S. Foerster, A. Kornowski, C. Klinke and H. Weller, *Science*, 2010, **329**, 550-553.
3. G. Konstantatos and E. H. Sargent, *Nat. Nanotechnol.*, 2010, **5**, 391-400.
4. X. Fang, Y. Bando, M. Liao, T. Zhai, U. K. Gautam, L. Li, Y. Koide and D. Golberg, *Adv. Funct. Mater.*, 2010, **20**, 500-508.
5. V. Sukhovatkin, S. Hinds, L. Brzozowski and E. H. Sargent, *Science*, 2009, **324**, 1542-1544.
6. C. Sun, N. Mathews, M. Zheng, C. H. Sow, L. H. Wong and S. G. Mhaisalkar, *J. Phys. Chem. C*, 2009, **114**, 1331-1336.
7. N. Mathews, B. Varghese, C. Sun, V. Thavasi, B. P. Andreasson, C. H. Sow, S. Ramakrishna and S. G. Mhaisalkar, *Nanoscale*, 2010, **2**, 1984-1998.
8. X. Gong, M. Tong, Y. Xia, W. Cai, J. S. Moon, Y. Cao, G. Yu, C.-L. Shieh, B. Nilsson and A. J. Heeger, *Science*, 2009, **325**, 1665-1667.
9. Y. Che, X. Yang, G. Liu, C. Yu, H. Ji, J. Zuo, J. Zhao and L. Zang, *J. Am. Chem. Soc.*, 2010, **132**, 5743-5750.
10. T. Mueller, F. Xia and P. Avouris, *Nat. Photonics*, 2010, **4**, 297-301.
11. X. Fang, Y. Bando, M. Liao, U. K. Gautam, C. Zhi, B. Dierre, B. Liu, T. Zhai, T. Sekiguchi, Y. Koide and D. Golberg, *Adv. Mater.* , 2009, **21**, 2034-2039.
12. L. Hu, L. Wu, M. Liao and X. Fang, *Adv. Mater.* , 2011, **23**, 1988-1992.
13. T. Zhai, H. Liu, H. Li, X. Fang, M. Liao, L. Li, H. Zhou, Y. Koide, Y. Bando and D. Golberg, *Adv. Mater.* , 2010, **22**, 2547-2552.
14. L. Li, X. Fang, T. Zhai, M. Liao, U. K. Gautam, X. Wu, Y. Koide, Y. Bando and D. Golberg, *Adv. Mater.* , 2010, **22**, 4151-4156.
15. P. Hu, Z. Wen, L. Wang, P. Tan and K. Xiao, *ACS Nano*, 2012, **6**, 5988-5994.
16. J. T. Yates, *Science*, 1998, **279**, 335-336.
17. L. Guo, E. Leobandung and S. Y. Chou, *Science*, 1997, **275**, 649-651.
18. A. Blanco, E. Chomski, S. Grabtchak, M. Ibisate, S. John, S. W. Leonard, C. Lopez, F. Meseguer, H. Miguez, J. P. Mondia, G. A. Ozin, O. Toader and H. M. van Driel, *Nature*, 2000, **405**, 437-440.
19. X. Chen, C. Li and K. Tsang Hon, *NPG Asia Mater.*, 2011, **3**, 34-40.
20. P. Fan, U. K. Chettiar, L. Cao, F. Afshinmanesh, N. Engheta and M. L. Brongersma, *Nat. Photonics*, 2012, **6**, 380-385.
21. A. I. Hochbaum, R. Chen, R. D. Delgado, W. Liang, E. C. Garnett, M. Najarian, A. Majumdar and P. Yang, *Nature*, 2008, **451**, 163-167.
22. V. S.-Y. Lin, K. Motesharei, K.-P. S. Dancil, M. J. Sailor and M. R. Ghadiri, *Science*, 1997, **278**, 840-843.
23. D. D. D. Ma, C. S. Lee, F. C. K. Au, S. Y. Tong and S. T. Lee, *Science*, 2003, **299**, 1874-1877.
24. D. H. Auston, P. Lavallard, N. Sol and D. Kaplan, *Appl. Phys. Lett.*, 1980, **36**, 66-68.
25. S. G. Chamberlain and J. P. Y. Lee, *IEEE J SOLID-ST CIRC*, 1984, **19**, 41 - 48
26. Z. Huang, J. E. Carey, M. Liu, X. Guo, E. Mazur and J. C. Campbell, *Appl. Phys. Lett.*, 2006, **89**, 033506-033503.
27. M. Y. Liu, E. Chen and S. Y. Chou, *Appl. Phys. Lett.*, 1994, **65**, 887-888.
28. S.-W. Hwang, H. Tao, D.-H. Kim, H. Cheng, J.-K. Song, E. Rill, M. A. Brenckle, B. Panilaitis, S. M. Won, Y.-S. Kim, Y. M. Song, K. J. Yu, A. Ameen, R. Li, Y. Su, M. Yang, D. L. Kaplan, M. R. Zakin, M. J. Slepian, Y. Huang, F. G. Omenetto and J. A. Rogers, *Science*, 2012, **337**, 1640-1644.
29. G. Konstantatos, J. Clifford, L. Levina and E. H. Sargent, *Nat. Photonics*, 2007, **1**, 531-534.
30. A. Zhang, H. Kim, J. Cheng and Y.-H. Lo, *Nano Lett.*, 2010, **10**, 2117-2120.
31. X. Gong, M. Tong, Y. Xia, W. Cai, J. S. Moon, Y. Cao, G. Yu, C.-L. Shieh, B. Nilsson and A. J. Heeger, *Science* 2009, **325**, 1665-1667.
32. O. Yaffe, L. Scheres, S. R. Puniredd, N. Stein, A. Biller, R. H. Lavan, H. Shpaisman, H. Zuilhof, H. Haick, D. Cahen and A. Vilan, *Nano Lett.*, 2009, **9**, 2390-2394.
33. X. C. Dou, G. H. Li and H. C. Lei, *Nano Lett.*, 2008, **8**, 1286-1290.
34. Y. Wu, R. Fan and P. Yang, *Nano Lett.*, 2002, **2**, 83-86.